Available online at www.sciencedirect.com

ScienceDirect

Procedia CIRP 74 (2018) 553–556

www.elsevier.com/locate/procedia

10th CIRP Conference on Photonic Technologies [LANE 2018]

Temperature distribution during laser based heat conduction welding of CFRP

V. Wippo[a,*], Y. Winter[a], P. Jaeschke[a], O. Suttmann[a], S. Kaierle[a], L. Overmeyer[a]

[a]*Laser Zentrum Hannover e.V., Hollerithallee 8, 30419 Hannover, Germany*

* Corresponding author. Tel.: +49-511-2788384 ; fax: +49-511-2788-100. *E-mail address:* v.wippo@lzh.de

Abstract

For the implementation of carbon fiber reinforced (CFRP) parts, these need to be assembled to more complex structures. Therefore, laser transmission welding was transferred to heat conduction welding for joining thermoplastic CFRP to itself. The goal of these investigations was to determine the influence of the focal point geometry and the main fiber orientation within the CFRP on the temperature distribution at the upper joining member. A set-up was chosen consisting of two thermo cameras in order to measure the process temperatures on top and underneath the upper joining member. Furthermore, the heat affected width was determined and correlated to the process temperatures.

Keywords: heat conduction welding; contour welding; thermoplastic; carbon fiber; process temperture, seam strength

1. Introduction

Today, carbon fiber reinforced materials are used for many different applications in order to implement the newest light weight design. This is the reason that the carbon fiber market has grown in the last couple years. Based on the year 2010, the carbon fiber demand increased by 11.5% each year. [1]

Due to the increase of CFRP usage also the process-know-how as well as understanding of the characteristic of the CFRP itself increased, so further applications are possible. For many applications it is necessary to join CFRP parts to other CFRP parts. This can be done by adhesive bonding or riveting. When the CFRP consists of a thermoplastic matrix welding techniques can be applied such as vibration, ultrasonic and induction welding. [2] Another new welding techniques is laser based heat conduction welding, which is a progression of the laser transmission welding. [3] At the classic laser transmission welding the laser radiation passes the upper joining member and is absorbed at the lower joining member, where the heat development takes place. Due to heat conduction between the parts the upper joining member becomes molten, too and after resolification a weld seam is generated. This welding technique can only be applied when the upper joining member is transparent or partly transparent for the laser radiation such as natural polymers. [4,5] If the upper joining member contains carbon fibers the radiation is absorbed directly at the carbon fibers, so the laser radiation cannot pass the upper part. This effect is used at the laser based heat conduction welding.

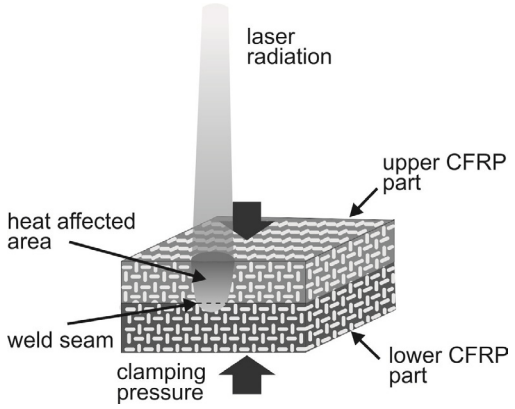

Fig. 1. Priciple of heat conduction welding of CFRP.

10.1016/j.procir.2018.08.115

The process heat is generated at the surface of the upper joining member and due to heat conduction the lower part becomes molten too. [3]

It is important for this joining method that enough heat is generated so the lower part is molten, but the surface of the upper part becomes not damaged by the heat generation. In order to enhance the understanding of heat conduction welding of CFRP, the influence of the focal point geometry on the process temperature generation and the resulting seam strength need to be known.

Nomenclature

T_g	glass transition temperature
T_m	melting temperature
T	temperature
A…	focal point geometry
B…	…focal point geometry
ΔT_{bot}	temperature difference on the bottom of the CFRP
ΔT_{top}	temperature difference on the top of the CFRP
HAW	heat affected width
ΔHAW_{bot}	difference in HAW on the bottom of the CFRP
ΔHAW_{top}	difference in HAW on top of the CFRP
α, β	detection angle
E_s	energy per unit length

2. Experimental Set-up

The experiments were conducted with carbon fiber fabric reinforced PPS (CETEX) produced by Tencate Advanced Composites BV with a fiber volume of 50%. PPS is a semicrystalline thermoplastic. The glass transmission temperature of natural PPS is T_g = 85-95°C and the melting point is T_m = 285-290°C. For a short time frame PPS can be used at T = 270-300°C and permanent at T = 200-240°C. It is known for its fire resistance, stiffness and resistance to chemicals. [6] The matrix material is natural, so it is transparent for NIR-radiation. The carbon fiber fabric has a 5 Harnes weave style and the lay-up is (0,90)/(90,0). The CFRP laminate consists of two carbon fiber fabric layers and has a total thickness of d = 0.62 mm.

All experiments were conducted with a main fiber orientation parallel to the weld seam path. For the heat conduction welding a diode laser emitting at λ = 940 nm was used. The maximum output power was P = 300 W. The experiments were conducted with a welding head generating a homogenized focal point with the dimension of 10 x 10 mm² to 10 x 20 mm². The test samples were moved by an axis system relatively to the welding head.

In order to determine the process temperatures of the upper part, two thermo cameras were used to determine the temperatures of the surfaces of the CFRP (Figure 2). The upper thermo camera was placed at an angle of α = 68° relative to the surface of the CFRP. The lower thermo camera was placed in an angle of β = 90° to the surface. The thermo camera forms a 2D pseudocolor image representing the temperature values. For the evaluation of the thermo camera images, the maximum temperatures were determined, which occur during the welding process. Furthermore, a straight measuring line was placed perpendicular to the axis feed in the area where the highest temperatures occur. Then the maximum temperature for each pixel on this line was determined and a corresponding envelope was created.

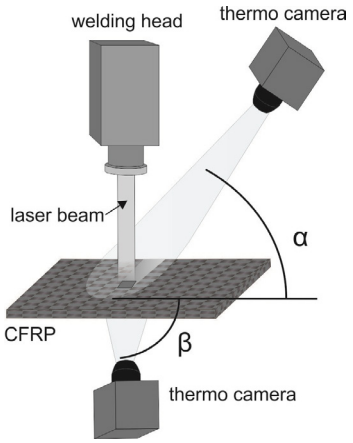

Fig. 2. Set-up used for the detection of the welding temperatures on top and underneath the CFRP.

For the evaluation of the weld seam strength overlap, samples were welded and t tested with a tensile testing machine. Furthermore, the weld seam area was measured in order to determine the average weld seam width of each sample. All experiments were conducted by contour welding. Pre-tests were performed in order to determine the welding speed depending on the laser power needed to join materials. The maximum welding speed was defined, when a continuous weld seam was generated. The minimum welding speed was set when visible damage of the matrix material occurred due to process temperatures that were too high.

3. Results and Discussion

For the evaluation of the maximum weld seam temperatures, the experiments were conducted with a constant laser power of P = 9 W and varying welding speed between v = 13-27 mm/min in order to generate different energy per unit length E_S the minimum welding speed was set to the point when the matrix material on the surface of the upper joining member started to degenerate while the carbon fibers remain nearly unharmed. The maximum welding speed was set to the point when only a small but continuous heat affected was generated underneath the CFRP.

The laser beam width was always 10mm and the length was 10mm (A) and 20mm (B), respectively. In Fig. 3 are shown the maximum temperatures for two different spot sizes. The focal point geometry with A=10x10mm² generates higher temperatures on top and underneath the CFRP than the focal point geometry of B=10x20mm². This is due to the twice as high radiation density in combination with half as long interaction time between the radiation and the CFRP. So for the process with focal point B a longer time frame is available in which the process heat can dissipate out of the processing area. Furthermore, it was not possible to generate a heat affected area only with the focal point A for E_s = 36 J/mm without damaging (smoke development) the surface.

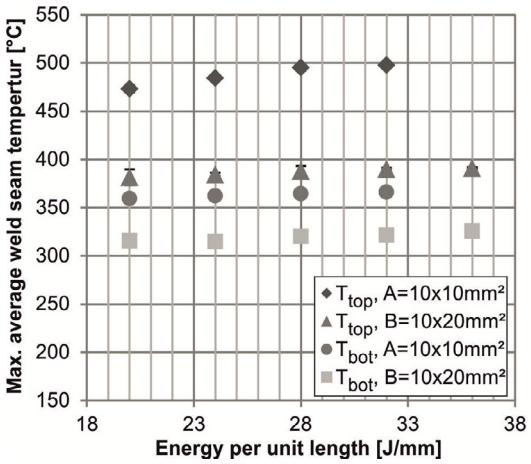

Fig. 3. Max. average weld seam temperatures for welding with two different focal point geometries.

The difference in the temperatures on top the CFRP generated by the different focal point geometries is at $E_S = 20$ J/mm $\Delta T_{top} = 91.4$ K. The difference of the temperatures underneath the CFRP is $\Delta T_{bot} = 43.7$ K and so clearly lower than the one of the upper surface. This difference can be deducted to the heat conduction from the surface into the material thickness, which has more time to take place for the focal point geometry B resulting in a lower temperature loss than for the focal point A.

In Figure 4 are depicted the average heat affected width for the two focal point geometries. The difference of the heat affected width on top and underneath the CFRP is similar with $\Delta HAW_{top} = 1.7$mm and $\Delta HAW_{bot} = 1.9$mm at $E_s = 20$ J/mm. Furthermore, due to the detected temperatures it was expected that the upper heat affected width for the focal point geometry B is larger than the lower heat affected width for the focal point geometry A, which is not the case.

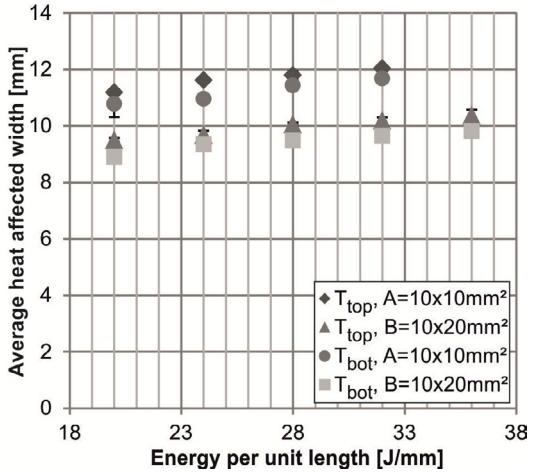

Fig. 4. Average heat affected width on top and bottom for the focal point geometries A and B.

This indicated that not only the maximum temperatures are the only factor influencing the HAW, but also another factor such as the exact temperature distribution. In order to determine the temperature distribution a measurement line was placed perpendicular to the weld seam orientation in the area with the highest temperatures in the thermo camera image. Then the maximum temperatures over the bead on plate welding process for each pixel on the measurement line were determined. Furthermore, the envelope curves for the temperatures on top the CFRP were corrected in order to compensate the different detection angle of the thermo camera compared to the camera detecting the temperatures underneath.

The resulting envelope curves are shown in Figure 5. The envelope curve for the maximum temperatures on top of the CFRP and for the focal point geometry B increases faster than for the temperatures from underneath the CFRP and for focal point A. This results in a smaller seam width, which is generated due to the melting of the matrix material.

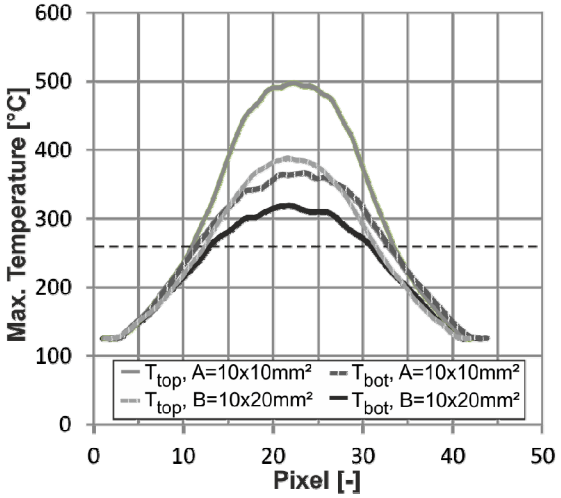

Fig. 5. Envelope curves of the maximum temperatures at Es = 32 J/mm.

In a next step, overlap samples were welded and tested. Therefore, the welding speed and so the welding range was determined for two different laser powers (45W, 60W
) for both focal point geometries. The maximum welding speed, and so the minimum energy per unit length, was set to the point when a continuous weld seam was generated. The minimum welding speed resulting in the maximum energy per unit length was set to the point when the matrix material on the surface of the upper parts starts to show signs of degradation.

The weld seam strength increases for higher energy per unit length for all combinations (Figure 6). This corresponds with the increase of the weld seam width (Figure 7). The welding process with the focal point geometry A and P = 60 W needed less energy per unit length than the other combinations in order to generate a continuous weld seam. Furthermore, the welding range for this combination is smaller than for the others. The welding range for the focal point A at P = 45 W is almost the same than for the focal point geometry B at P = 60 W. This based on the different heat generation as described before. The largest welding range was obtained with the focal point geometry B and P = 45 W, which generated the highest seam strength with 8.8 kN.

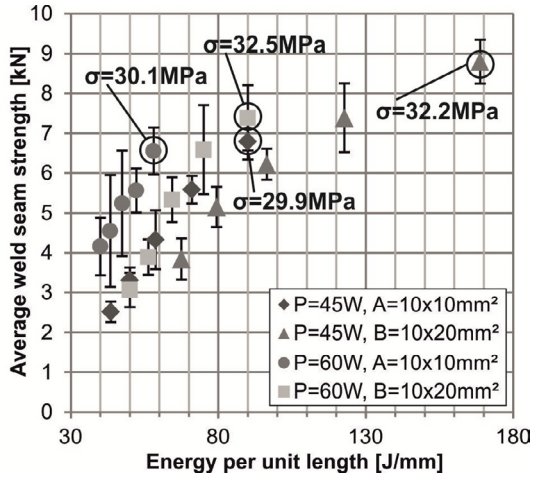

Fig. 6. Average seam strength for the focal point geometries A and B at different energy per unit length.

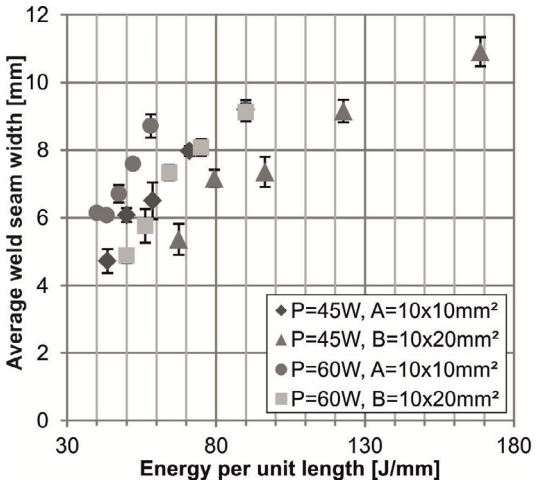

Fig. 7. Average weld seam width for the focal point geometries A and B at different energy per unit length.

Besides the seam strength, also the weld seam width increases, which correlates with the results of the previous investigations. This time there is a second part, into which the process heat conducts and does not remain only in the upper parts to melt the thermoplastic. The increase of the weld seam width affects the overall shear strength, which is the ratio between seam strength to weld seam area. The shear strength was calculated for the parameters generating the highest seam strengths. The resulting seam strengths for all parameter combinations are similar, which leads to the deduction, that for a process development the process with the highest welding speed can be chosen. Furthermore, less space at the part is needed for the weld seam generation. If the overall strength of the weld seam is the main criteria, the parameter with the focal point geometry B and P = 45 W should be chosen.

Conclusions

Investigations were carried out on the process heat development at heat conduction welding of CFRP. The focal point geometry, especially the focal point length parallel to the weld seam, affect the heat development. At $E_S = 20$ J/mm the difference in the temperature is $\Delta T_{top} = 91.4$ K on top of the CFRP and $\Delta T_{bot} = 43.7$ K on the bottom of the CFRP just due to the focal point. This also affects the resulting HAW with $\Delta HAW_{top} = 1.7$mm and $\Delta HAW_{bot} = 1.9$mm at $E_s = 20$ J/mm.

Furthermore, overlap samples were welded and tested for their strength. The highest seam strength was generated with the focal point geometry B and a laser power of P = 45 W. The shear strength for 4 different processing parameters was between σ = 29.9 MPa and σ = 32.5MPa.

In order to enhance the understanding of this new welding process further investigations have to be performed focusing on the material influences such as material composition and material thickness. At the welding of higher material thicknesses probably more process heat would be needed, because more material is available into which the heat can conduct.

The heat conduction welding would allow using this welding technique to join large CFRP structures such as used in the aerospace industry.

Acknowledgements

The authors thank the Federal Ministry for Economic Affairs and Energy (BMWI) for funding these investigations within the project InduLas (ZF4102310FH6).

References

[1] Witten E., Kraus T., Kuehnel M. Composites-Marktbericht 2015, Carbon Composites e.V. & AVK-Verlag. 2015

[2] Fernandez Villegas I., Moser L., Yousefpour A., Mitschang P., Bersee H.EN: Process and performance evaluation of ultrasonic, induction and resistance welding of advanced thermoplastic composites. Journal of Thermoplastic Composite Materials 26(8) 1007–1024, 2012

[3] Wippo V., Ihde J., Jaeschke P., Linde P., Suttmann O., Overmeyer L.: Laser heat conduction welding of inline cleaned endless carbon fibre reinforced thermoplastics. In: 17th European conference on composite materials, Munich, Germany, 2016

[4] Jaeschke P.: Laserdurchstrahlschweißen kontinuierlich kohlenstofffaser-verstärkter Kunststoffe und thermoplastischer Polymere. Dissertation. Leibniz Universität Hannover. 2012

[5] Frick T.: Untersuchung der prozessbestimmenden Strahl-Stoff-Wechsel-wirkungen beim Laserschweißen von Kunststoffen. Bamberg: Meisenbach. 2007

[6] Ehrenstein G.W.: Faserverbund-Kunststoffe. Werkstoffe- Verarbeitung-Eigenschaften. Carl Hanser Verlag München Wien. 2006.